



Estimating temperatures in refrigerated containers and trailers

How many randomly-placed cargo temperature sensors are necessary?

dr. L.J.S. (Leo) Lukasse, drs. ing. J.C.M.A. (Joost) Snels



WAGENINGEN
UNIVERSITY & RESEARCH

Estimating temperatures in refrigerated containers and trailers

How many randomly placed cargo temperature sensors are necessary?

Authors: dr. L. (Leo) Lukasse, drs.ing. J. (Joost) Snels

Institute: Wageningen Food & Biobased Research

This study was carried out by Wageningen Food & Biobased Research, subsidised by the Dutch Ministry of Agriculture, Nature and Food Quality, funded by NWO and commissioned by Wageningen Food & Biobased Research.

Wageningen Food & Biobased Research
Wageningen, April 2022

Public

Report 2279

DOI <https://doi.org/10.18174/568806>

WFBR Project number: 6230188100

Version: Final

Reviewer: dr.ir. C.V.C. (Caspar) Geelen

Approved by: dr.ir. H. (Henk) Wensink

Carried out by: Wageningen Food & Biobased Research

Subsidised by: the Dutch Ministry of Agriculture, Nature and Food Quality

Funded by: NWO

Commissioned by: Wageningen Food & Biobased Research

This report is: Public

This publication is part of the project quality controlled Logistics in IoT-enabled Perishable Supply Chains (439.19.609) of the research programme Accelerator - Kennis en innovatie voor een concurrerende logistieke sector which is (partly) financed by the Dutch Research Council (NWO)

The research that is documented in this report was conducted in an objective way by researchers who act impartial with respect to the client(s) and sponsor(s). This report can be downloaded for free at <https://doi.org/10.18174/568806> or at www.wur.eu/wfbr (under publications).

© 2022 Wageningen Food & Biobased Research, institute within the legal entity Stichting Wageningen Research.

The client is entitled to disclose this report in full and make it available to third parties for review.

Without prior written consent from Wageningen Food & Biobased Research, it is not permitted to:

- a. partially publish this report created by Wageningen Food & Biobased Research or partially disclose it in any other way;
- b. use this report for the purposes of making claims, conducting legal procedures, for (negative) publicity, and for recruitment in a more general sense;
- c. use the name of Wageningen Food & Biobased Research in a different sense than as the author of this report.

PO box 17, 6700 AA Wageningen, The Netherlands, T + 31 (0)317 48 00 84, E info.wfbr@wur.nl, www.wur.eu/wfbr.

All rights reserved. No part of this publication may be reproduced, stored in a retrieval system of any nature, or transmitted, in any form or by any means, electronic, mechanical, photocopying, recording or otherwise, without the prior permission of the publisher. The publisher does not accept any liability for inaccuracies in this report.

Contents

| | | |
|----------|---|-----------|
| | Summary | 4 |
| 1 | Introduction | 5 |
| 2 | Physical model | 6 |
| 2.1 | Air flow rate and distribution of air flow over the zones | 10 |
| 2.2 | Heat transfer coefficient K and distribution over the zones | 11 |
| 2.3 | balances for return - and supply air temperature | 12 |
| 3 | Statistical model | 14 |
| 4 | Case study | 15 |
| 4.1 | The studied transport scenario | 15 |
| 4.2 | The studied sensor-placement methods | 17 |
| 4.3 | Evaluation criteria | 17 |
| 4.4 | Evaluated simulations | 23 |
| 5 | Results | 24 |
| 5.1 | Random sensor placement | 24 |
| 5.2 | deterministic sensor placement | 26 |
| 6 | Discussion | 27 |
| 6.1 | Required number of sensors | 27 |
| 6.2 | Deterministic sensor placement | 27 |
| 6.3 | Economic value | 28 |
| 6.4 | Applicability to refrigerated trailers | 28 |
| 6.5 | Mechanistic or statistical model? | 29 |
| 7 | Conclusions | 30 |
| 8 | Recommendations | 31 |
| | Literature | 32 |

Summary

How many randomly placed cargo temperature sensors are necessary to gain a sufficiently accurate estimate of the temperatures of the complete cargo during refrigerated transport in reefer containers and (single compartment) refrigerated trailers?

To answer the above question it is necessary to first determine what exactly the actual temperature profile in a standard container is. To that end a physical model of the temperature dynamics in reefer containers and refrigerated trailers was constructed. The model has not been validated explicitly, but the simulation outcomes compare reasonably well with what the authors, experts on temperature management during refrigerated transport, would expect. This physical model is then simulated for a reefer container shipment scenario representative of a banana transport. The scenario includes a pulldown phase because it assumes stuffing non-precooled bananas. Then a statistical model of the temperature distribution in a reefer container is defined. Inputs of the statistical model are any number of cargo temperature measurements collected at unknown locations in the cargo space. The statistical model simply calculates the cumulative distribution function of the measurements, without making any assumption about the type of distribution function. The difference between the statistical model output and the physical model output is analysed for a range of sensor numbers and different sensor-placement methods.

The results indicate that there is little benefit in placing more than 30 randomly placed sensors per container load for the purpose of gaining a sufficiently accurate estimate of the temperatures of the complete cargo during refrigerated transport in reefer containers, when using these recordings as inputs for a statistical model.

It is not to be expected that the situation will be a lot different for refrigerated trailers, because there is no radical difference between refrigerated trailers and containers in terms of equipment size or in terms of the typically occurring pattern of temperature distribution.

Care should be taken, as the conclusions depend on many assumptions.

Random sensor placement is an ineffective sensor placement method, as two smartly placed sensors can be more informative than *e.g.* 40 randomly placed sensors. Smart sensor placement in a container is: one in the bottom of the coldest pallet (position 2 or 3 from unit-end) and one in the centre of the warmest pallet (door-end).

The main research question in this study is very generic, and therefore hard to answer adequately. For future studies it is recommended to be more specific in formulating the purpose and application domain of temperature recording during transport.

1 Introduction

This study seeks to answer the following main question:

How many randomly placed cargo temperature sensors are necessary to gain a sufficiently accurate estimate of the temperatures of the complete cargo during refrigerated transport in reefer containers and (single compartment) refrigerated trailers?

Background of the question is the idea to routinely equip a part of the crates with temperature sensors to reconstruct the cargo temperatures after each shipment. Assuming that there is no control over the positioning of those crates in the complete cargo of 1000+ crates, which percentage of the crates should be equipped with sensors?

Though the question sounds simple, answering it involves many debatable choices and assumptions.

Some of the difficult choices:

1. What is an appropriate unit of measure for the 'estimate of the temperatures of the complete cargo'?
2. How to judge if an estimate is 'sufficiently accurate'?

Despite these difficulties this manuscript seeks to answer the main question (see box above).

Some of the assumptions made:

1. The position of the randomly placed cargo temperature sensors is unknown.
2. Limit the scope to palletized full load shipments of one type of cargo (no mix loads, no part loads, no hand-stowed cargo).
3. Focus on chilled transport (setpoint > -5 °C) of fruit and vegetable, where autonomous heat production and the accompanying risk of heated pallet load centres exists.
4. Cargo is not necessarily pre-cooled at start of trip.
5. Let's focus on warm ambient temperature of 30 °C.

In order to determine how many randomly placed temperature sensors are required to accurately reconstruct the entire temperature profile in the container and its cargo, it is necessary to first determine what exactly the actual temperature profile in a standard container is. Therefore, in section 2 a physical model is developed to be as accurately as possible a representation of the true temperature distribution in a reefer. The model is constructed in such a fashion that its parameters can be adjusted to suit the type of trailer or container as well as its cargo specifics, thus the method will be applicable to various types of containers as well as cargo types, amounts and patterns of loading. The model is not validated explicitly, but the simulation outcomes are compared to what the authors, experts on temperature management during refrigerated transport, would expect. Secondly in section 3 the statistical model is defined.

Thirdly in section 4 it is described how the statistical model outputs are compared to the true temperature distribution (*i.e.*, the physical model outputs) to answer this manuscript's main question on the needed number of temperature sensors (see box above). Section 5 then presents the results of this comparison, which are discussed in section 6. Finally, the study leads to the conclusions and recommendations listed in respectively sections 7 and 8.

2 Physical model

Figure 1 sketches a reefer container. The positions of the return air temperature sensor and the supply air temperature sensor are indicated in the figure.

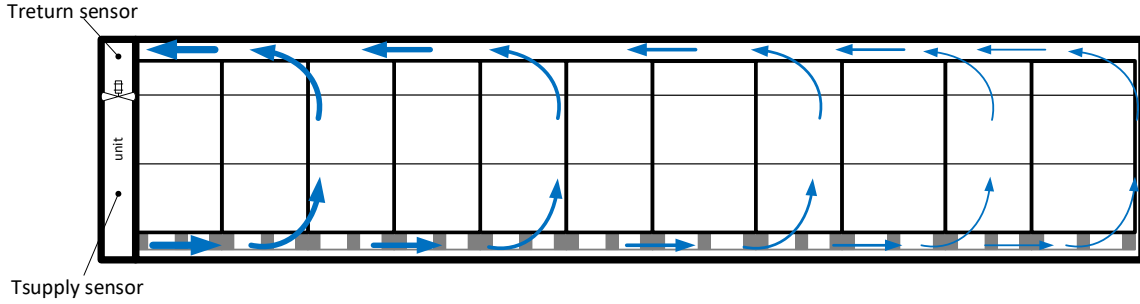


Figure 1 *schematic presentation of reefer container*

The physical model discretizes the cargo space in multiple imaginary zones as illustrated in Figure 2 to account for the, usually dominant, temperature gradient in longitudinal direction. A natural choice is to dimension the model zones such that each zone contains two pallets next to each other. Within each zone the model distinguishes between air and pallet load. Each pallet load is then divided in multiple imaginary concentric layers to take into account that the temperature gradients within a pallet load can be significant (Figure 2).

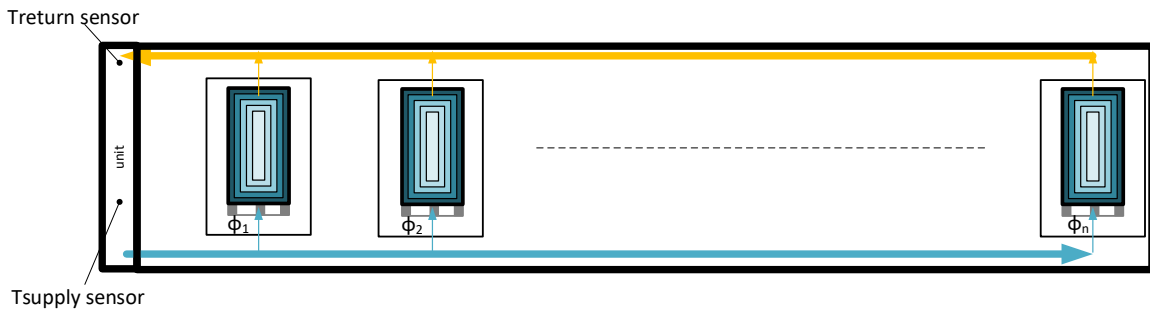


Figure 2 *schematic representation of zonal model, distinguishing between air and pallet load temperature, accounting for temperature gradients within pallet load*

The heat balance for air in each zone z is

$$\frac{1000}{3600} \times m_{air,z} \times c_{p,air} \times \frac{dT_{air,z}(t)}{dt} = \frac{\phi_z}{3600} \times \rho_{air} \times 1000 \times c_{p,air} \times (T_{sup}(t) - T_{air,z}(t)) + n_{pallets_per_zone} \times Q_{out,nlayers}(t) + U_z \times (T_{amb}(t) - T_{air,z}(t)) \quad [W] \quad (1)$$

Note that all model variables used in this section are defined in Table 1. The sum of all zonal air flow rates ϕ_z equals the supply air flow rate delivered by the refrigeration unit (manufacturer's spec):

$$\phi_{unit} = \sum_{z=1}^{n_{zones}} \phi_z \quad [m^3/h] \quad (2)$$

The sum of all zonal heat ingresses equals the container's overall heat ingress according to:

$$U_{total} = \sum_{z=1}^{n_{zones}} U_z \quad [W \cdot m^{-2} \cdot K^{-1}] \quad (3)$$

where heat loss coefficient U_{total} relates to the overall heat transfer coefficient K_{total} and

$$U_{total} = K_{total} \times A_{total} \quad [W \cdot m^{-2} \cdot K^{-1}] \quad (4)$$

K_{total} is a manufacturer's spec.

To define the heat balance for a model layer of the pallet load first the surface areas of these layers needs to be calculated. Pallet loads are shaped like rectangular cuboids. The surface area and volume of such bodies is given by:

$$A_{pl} = 2 \times (L_{pl} \times W_{pl} + L_{pl} \times H_{pl} + W_{pl} \times H_{pl}) \quad [\text{m}^2] \quad (5)$$

And

$$V_{pl} = L_{pl} \times W_{pl} \times H_{pl} \quad [\text{m}^3] \quad (6)$$

In the model we divide these rectangular cuboids in n_{layers} imaginary concentric rectangular cuboids (see Figure 3 for a schematic 2D representation).

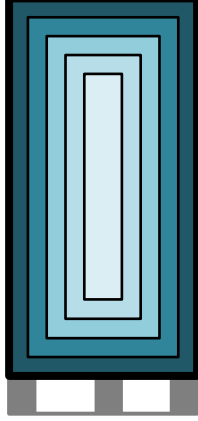


Figure 3 2D presentation of pallet load imaginarily divided in concentric rectangular cuboids

Let layer 1 by the inner layer and layer n_{layers} the outer layer, where all layers are equally thick, then the thicknesses d_L , d_W and d_H of the layers in all three directions are:

$$d_L = \frac{L_{pl}}{2n_{layers}}, d_W = \frac{W_{pl}}{2n_{layers}}, d_H = \frac{H_{pl}}{2n_{layers}} \quad [\text{m}] \quad (7)$$

While length L_l , width W_l and height H_l of the outer surface of layer l are

$$L_l = 2 \times d_L \times l, W_l = 2 \times d_W \times l, H_l = 2 \times d_H \times l \quad [\text{m}] \quad (8)$$

After which the outer area of layer l is given by

$$A_l = 2 \times (L_l \times W_l + L_l \times H_l + W_l \times H_l) \quad [\text{m}^2] \quad (9)$$

The volume of layer 1 is given by

$$V_1 = L_1 \times W_1 \times H_1 \quad [\text{m}^3] \quad (10)$$

And the volume of all other layers is given by

$$V_l = L_l \times W_l \times H_l - L_{l-1} \times W_{l-1} \times H_{l-1} \quad [\text{m}^3] \quad (11)$$

The heat balance for pallet load layer l in model zone z is

$$\frac{1000}{3600} \times V_l \times \rho_{pl} \times c_{p,pl} \times \frac{dT_l(t)}{dt} = Q_{in,l}(t) - Q_{out,l}(t) + Q_{prod,l} \quad [\text{W}] \quad (12)$$

Where

$$Q_{prod,l} = V_l \times \rho_{pl} \times q_{prod}^{spec}/1000 \quad [\text{W}] \quad (13)$$

And

$$Q_{in,l}(t) = \begin{cases} 0 & \text{if } l = 1 \\ \lambda \times \left(\frac{2 \times H_{l-1} \times W_{l-1}}{d_L} + \frac{2 \times W_{l-1} \times L_{l-1}}{d_H} + \frac{2 \times L_{l-1} \times H_{l-1}}{d_W} \right) \times (T_{l-1} - T_l) & \text{if } l > 1 \end{cases} \quad [\text{W}] \quad (14)$$

And

$$Q_{out,l}(t) = \begin{cases} \lambda \times \left(\frac{2 \times H_l \times W_l}{d_L} + \frac{2 \times W_l \times L_l}{d_H} + \frac{2 \times L_l \times H_l}{d_W} \right) \times (T_l(t) - T_{l+1}(t)) & \text{if } l < n_{layers} \\ \left(\alpha_{pa} \times (2 \times H_l \times W_l + 2 \times W_l \times L_l + 2 \times L_l \times H_l) + \lambda \times \left(\frac{2 \times H_l \times W_l}{0.5 \times d_L} + \frac{2 \times W_l \times L_l}{0.5 \times d_H} + \frac{2 \times L_l \times H_l}{0.5 \times d_W} \right) \right) \times (T_l(t) - T_{air,z}(t)) & \text{if } l = n_{layers} \end{cases} \quad [W] \quad (15)$$

In the above equation $Q_{out,l}$ for $l = n_{layers}$ describes the heat flow from the pallet load's outer layer to the air in zone z.

Assumptions:

1. The above heat balance ignores the possible effect of transpiration.
2. Assumes an equal airflow rate along all sides of all pallets in a zone.
3. Assumes that air temperature around the pallet is everywhere the same.
4. No air flow through the pallet load.
5. Pallet load is a uniform medium (*i.e.*, a uniform mix of packaging materials, air, and cargo).
6. Stack effect (warm air has lower density and therefore tends to float to the top) ignored.

Table 1 nomenclature of model variables introduced in this section

| Variable | Description | Value | Unit |
|---------------|---|---|---------------------------------|
| α_{pa} | heat transfer coefficient between pallet load and air | [5, 25] (default: 10) | $W \cdot m^{-2} \cdot K^{-1}$ |
| λ | heat conduction coefficient of pallet load | for many fruits $0.2 < \lambda < 0.9$, water: 0.6 W/m/K , air: 0.024 W/m/K | $W \cdot m^{-1} \cdot K^{-1}$ |
| ρ_{air} | air density | 1.2 | kg/m^3 |
| ρ_{pl} | (bulk) density of pallet load, <i>i.e.</i> , pallet load weight divided by pallet load volume | avocado: 473, banana: 413, grape: 243 | kg/m^3 |
| ϕ_{unit} | air flow rate of refrigeration unit | 5000 | m^3/h |
| ϕ_z | air flow rate through zone z | - | m^3/h |
| A_l | outer surface area of model layer no. l | | m^2 |
| A_{pl} | outer surface area of a pallet load | | m^2 |
| A_{total} | surface area of container's insulated enclosure | | m^2 |
| $c_{p,air}$ | specific heat of air | 1.0 | $kJ \cdot kg^{-1} \cdot K^{-1}$ |
| $c_{p,pl}$ | specific heat of cargo (pallet loads), dominated by carried product | solid plastics = 1.67, paper = 1.34, ice = 2.09, water = 4.18 | $kJ \cdot kg^{-1} \cdot K^{-1}$ |
| d_H | thickness of a layer in vertical direction | - | m |
| d_L | thickness of a layer in longitudinal direction | - | m |
| d_W | thickness of a layer in transversal direction | - | m |
| H_l | height of outer surface of layer no. l | - | m |

| | | | |
|--------------------------|---|---|-------------------|
| H_{pl} | height of pallet load | 1.90 | m |
| K_{total} | heat transfer coefficient of total container | | $W.m^{-2}.K^{-1}$ |
| l | pallet model layer no. | $[1, n_{layers}]$ (1 = centre, n_{layers} = outer layer) | - |
| L_l | length of outer surface of layer no. l | - | m |
| L_{pl} | length of pallet load | 1.20 | m |
| $m_{air,z}$ | mass of air in zone z | | kg |
| n_{layers} | number of model layers (Figure 3) | - | - |
| $n_{pallets_per_zone}$ | no. of pallets per model zone | depends on zone length, by default 2 | - |
| n_{zones} | number of model zones (Figure 2) | - | - |
| q_{prod}^{spec} | autonomous heat production by cargo | [0, 60] | W/tonne |
| $Q_{in,l}(t)$ | heat flux into model layer l | | W |
| $Q_{out,l}(t)$ | heat flux out of model layer l | | W |
| $Q_{prod,l}(t)$ | heat production in model layer l | | W |
| t | time | | h |
| $T_{air,z}(t)$ | air temperature around pallet in zone z | | °C |
| $T_{amb}(t)$ | ambient air temperature | | °C |
| $T_l(t)$ | temperature of layer l | | °C |
| $T_{sup}(t)$ | supply air temperature | | °C |
| U_{total} | heat loss coefficient of insulated enclosure of total container | | $W.K^{-1}$ |
| U_z | heat loss coefficient of insulated enclosure of zone z | | $W.K^{-1}$ |
| V_l | volume of layer l | | m^3 |
| V_{pl} | volume of a pallet load | | m^3 |
| W_l | width of outer surface of layer no. l | - | m |
| W_{pl} | width of pallet load | 1.00 | m |
| z | zone no. | $[1, n_{zones}]$ (1 = unit-end zone, n_{zones} = door-end zone) | - |

2.1 Air flow rate and distribution of air flow over the zones

Table 2 lists the typical characteristics of containers and trailers as far as relevant to the subject of modelling temperature distribution.

Table 2 relevant typical characteristics of containers and trailers

| | container | trailer |
|--------------------------------------|---|---|
| no. of pallets (1.00 x 1.20 m) | 20 | 26 |
| maximum air flow rate ϕ_{total} | 5000 m ³ /h | 5000 m ³ /h |
| internal L x W x H | 11.60 x 2.29 x 2.54 m | 13.40 x 2.45 x 2.60 m |
| Typical K-value | 0.35 W.m ⁻² .K ⁻¹ | 0.40 W.m ⁻² .K ⁻¹ |
| location of air supply | bottom (Figure 1) | top (Figure 4) |

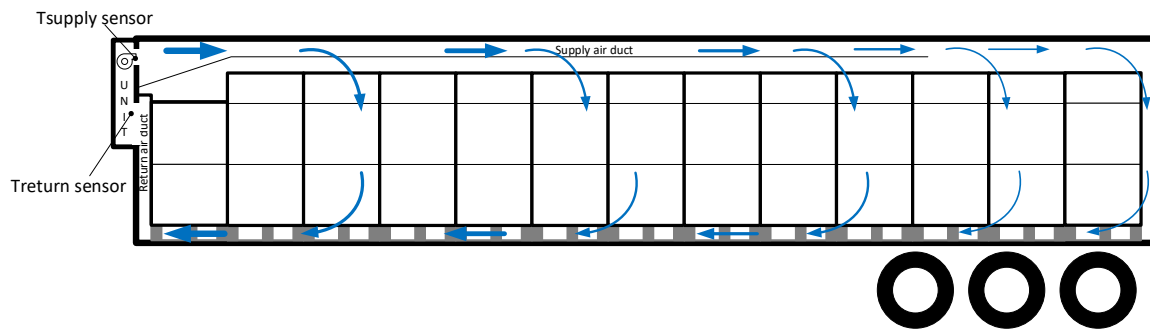


Figure 4 schematic presentation of refrigerated trailer

A container carries 20 pallets, and a trailer 26 (Table 2). Both in a container and in a trailer, there are always two pallets beside each other. In a trailer both are oriented transversally, while in a container one is placed transversally and one longitudinally. The natural choice is to choose one zone per two-pallets-beside-each-other, resulting in a zonal length L_z of 1.10 m in containers and 1.00 m in trailers. Table 3 proposes a default distribution of air flow over these zones. This proposal is based on confidential measurements of air velocities in a reefer container (Lukasse *et al.*, 2021a) and in a refrigerated trailer (Lukasse *et al.*, 2021b).

Table 3 default distribution of air flow over zones in % of airflow

| zone | containers | trailers |
|------|------------|----------|
| 1 | 7 | 4 |
| 2 | 18 | 11 |
| 3 | 18 | 11 |
| 4 | 16 | 11 |
| 5 | 12 | 10 |
| 6 | 8 | 9 |
| 7 | 6 | 9 |
| 8 | 5 | 8 |
| 9 | 5 | 8 |
| 10 | 5 | 6 |
| 11 | | 5 |
| 12 | | 4 |
| 13 | | 4 |

2.2 Heat transfer coefficient K and distribution over the zones

The overall heat transfer coefficient K_{total} of an insulated container or trailer depends on the K-value of the six individual wall panels according to

$$K_{total} = \frac{K_{wrf} \times A_{wrf} + K_{door} \times A_{door} + K_{unit} \times A_{unit}}{A_{wrf} + A_{door} + A_{unit}} \quad [\text{W.m}^{-2}.\text{K}^{-1}] \quad (16)$$

See Table 6 for a description of all variables newly introduced in section 2.2. Variables introduced in preceding sections are not repeated in Table 6. From earlier projects the impression is that for trailers roughly

$$K_{door} = K_{unit} = 3 \times K_{wrf} \quad [\text{W.m}^{-2}.\text{K}^{-1}] \quad (17)$$

while for containers, with usually thicker doors, this factor 3 is much closer to 1. Solve K_{wrf} from the above two equations to get

$$K_{wrf} = \frac{K_{total} \times (A_{wrf} + A_{door} + A_{unit})}{A_{wrf} + 3 \times A_{door} + 3 \times A_{unit}} \quad [\text{W.m}^{-2}.\text{K}^{-1}] \quad (18)$$

Knowing the length L , width W and height H of containers and trailers, and using the above equation K_{wrf} and K_{door} can be calculated individually, see Table 4.

Table 4 surface areas and K-value of wall panels for containers and trailers

| | container | trailer |
|--|-----------|---------|
| A_{door} [m ²] | 5.8 | 6.4 |
| A_{unit} [m ²] | 5.8 | 6.4 |
| A_{wrf} [m ²] | 112.1 | 135.3 |
| K_{wrf} [W.m ⁻² .K ⁻¹] | 0.29 | 0.35 |
| K_{door} [W.m ⁻² .K ⁻¹] | 0.88 | 1.02 |

The U-value of a zone is given by

$$U_z = \begin{cases} K_{wrf} \times (2 \times H + 2 \times W) \times L_z & \text{for } z = 1, \dots, n_{zones} - 1 \\ K_{wrf} \times (2 \times H + 2 \times W) \times L_z + K_{door} \times A_{door} & \text{for } z = n_{zones} \end{cases} \quad [\text{W.m}^{-2}.\text{K}^{-1}] \quad (19)$$

This equation with the inputs from Table 4 is the basis for Table 5. The values for containers in Table 5 do not exactly match the outcomes of the above equation, because they have been adjusted afterwards to make simulated temperatures match better with experience-based expected temperatures.

Table 5 distribution of U-value across zones in % of total U-value

| zone | containers | trailers |
|------|------------|----------|
| 1 | 9.9 | 6.5 |
| 2 | 9.9 | 6.5 |
| 3 | 9.9 | 6.5 |
| 4 | 9.9 | 6.5 |
| 5 | 9.9 | 6.5 |
| 6 | 9.9 | 6.5 |
| 7 | 9.9 | 6.5 |
| 8 | 9.9 | 6.5 |
| 9 | 9.9 | 6.5 |
| 10 | 10.9 | 6.5 |
| 11 | | 6.5 |
| 12 | | 6.5 |
| 13 | | 21.5 |

Table 6 nomenclature of model variables introduced in this section

| Variable | Description | Value | Unit |
|------------|---|-------|------------------------------------|
| A_{door} | surface area of rear doors | | m ² |
| A_{unit} | surface area of unit | | m ² |
| A_{wrf} | surface area of side Walls, Roof and Floor | | m ² |
| H | internal height of container | | m |
| K_{door} | heat transfer coefficient of rear doors | | W.m ⁻² .K ⁻¹ |
| K_{unit} | heat transfer coefficient of unit | | W.m ⁻² .K ⁻¹ |
| K_{wrf} | heat transfer coefficient of side Walls, Roof and Floor | | W.m ⁻² .K ⁻¹ |
| L | internal length of container | | m |
| L_z | length of model zone z | | m |
| W | internal width of container | | m |

2.3 balances for return - and supply air temperature

Transport refrigeration units typically record and/or control return air temperature T_{ret} and supply air temperature T_{sup} . To enable a connection between these recordings and the model it is good to extend the model with dynamic heat balances for T_{ret} and T_{sup} . The return air temperature sensor is located in the reefer unit's evaporator section. In close analogy with eqn. 1 the heat balance for the return air zone is

$$Q_{rp}(t) = \frac{1000}{3600} \times m_{rz} \times c_{p,rz} \times \frac{dT_{ret}(t)}{dt} = \frac{1}{3600} \times \rho_{air} \times 1000 \times c_{p,air} \times \phi_{unit} \times (T_{ru,in}(t) - T_{ret}(t)) + U_{fw} \times (T_{amb}(t) - T_{ret}(t)) + \quad [W] \quad (20)$$

with

$$T_{ru,in}(t) = \frac{\sum_{z=1}^{n_{zones}} (\phi_z \times T_{air,z}(t))}{\sum_{z=1}^{n_{zones}} \phi_z} \quad [^{\circ}C] \quad (21)$$

$$Q_{rp}(t) = U_{rp} \times (T_{air,1}(t) - T_{ret}(t)) \quad [W] \quad (22)$$

$$U_{fw} = 2 \times H \times W \times K_{total} \quad [W] \quad (23)$$

$$U_{rp} = 5 \times U_{fw} \quad [W] \quad (24)$$

See Table 7 for a description of all variables newly introduced in section 2.3. Variables introduced in preceding sections are not repeated in Table 7. The factor 2 in eqn. 23 is a rough approximation to account for the knowledge that container's front wall, in which the reefer unit is mounted, is usually worse insulated than the rest of the container. The factor 5 in eqn. 24 is an arbitrary choice to account for the fact that the rear panel is much worse, basically not, insulated than the front wall.

Note that $Q_{rp}(t)$ in eqn. 20 represents a heat flow through the reefer unit's Rear Panel from the air in model zone 1 to the reefer unit's evaporator compartment. To balance the equations a term $-Q_{rp}(t)$ is therefore added to the heat balance for the air in zone 1.

Effectively equation 20 predicts $T_{ret}(t) = T_{ru,in}(t)$ as long as the unit is powered up, and T_{ret} is between $T_{amb}(t)$ and $T_{cargospace}(t)$ when the unit is powered off.

For supply air temperature $T_{sup}(t)$ a merely empirically based first order differential equation is introduced:

$$\frac{dT_{sup}(t)}{dt} = \frac{1}{\tau_{Tsup}} \times (T_{sup,new}(t) - T_{sup}(t)) \quad [^{\circ}\text{C}] \quad (25)$$

with

$$T_{sup,new}(t) = \begin{cases} T_{set}(t) & \text{if } power = 1 \\ 0.7 \times T_{ret}(t) + 0.3 \times T_{air,1}(t) & \text{if } power = 0 \end{cases} \quad [^{\circ}\text{C}] \quad (26)$$

Table 7 *nomenclature of model variables introduced in this section*

| Variable | Description | Value | Unit |
|------------------|---|-------------------------------|--|
| τ_{Tsup} | time constant of 1 st order filter for T_{sup} | 0.1 | h |
| $c_{p,rz}$ | specific heat of metals in return air zone | aluminium = 0.9, copper = 0.4 | $\text{kJ}\cdot\text{kg}^{-1}\cdot\text{K}^{-1}$ |
| m_{rz} | mass of metals in reefer unit's evaporator compartment | 50 (estimate) | kg |
| $Q_{rp}(t)$ | heat flow Q through reefer unit's Rear Panel from cargo space to reefer unit's evaporator compartment | | |
| $T_{ret}(t)$ | return air temperature | | $^{\circ}\text{C}$ |
| $T_{ru,in}(t)$ | air temperature at inlet to refrigeration unit | | $^{\circ}\text{C}$ |
| $T_{set}(t)$ | setpoint temperature at time t | | $^{\circ}\text{C}$ |
| $T_{sup,new}(t)$ | newly calculated supply air temperature | | $^{\circ}\text{C}$ |
| U_{fw} | heat transfer coefficient of insulated front wall | | $\text{W}\cdot\text{K}^{-1}$ |
| U_{rp} | heat transfer coefficient of reefer unit's rear panel | $5 \cdot U_{fw}$ | $\text{W}\cdot\text{K}^{-1}$ |

3 Statistical model

In the statistical model it is assumed that a number of $N_{sensors}$ temperature sensors is placed in a batch of fruit. No further information is used: *i.e.*, no information about sensor locations, no information about the type of transport equipment (trailer or container), no information about the size of the contained space.

At any time t a number of $N_{sensors}$ measurements is collected in the batch. The statistical model simply uses these measurements (sample) to estimate the temperature distribution of the whole batch (population) at that same time t . This is done by calculating the cumulative distribution function of the measurements. First the $N_{sensors}$ measurements $T_{measured}(s,t)$ are sorted in ascending order, where $T_{measured}(s,t)$ is the temperature T measured by sensor s at time t . Then it is assumed that the chance of temperatures colder than or equal to $T_{measured}(s,t)$ is:

$$F_{stat}(T_{measured}(s,t)) = \frac{s}{N_{sensors}+1} \quad [-] \quad (27)$$

4 Case study

For one specific transport scenario the performance of the statistical model has been analysed for two sensor-placement methods. The studied transport scenario is described in section 4.1. The evaluated sensor-placement methods are described in section 4.2. The evaluation criteria to quantify the performance of the statistical model are defined in section 4.3.

4.1 The studied transport scenario

The studied transport scenario is a simulation run of the physical model (section 2). It concerns a container transport with a duration of 240 hours at setpoint 13.5 °C, initial cargo temperature 25 °C, autonomous heat production 20 W/tonne, a 12-hour power-off period between time 100 and 112 h, and an ambient temperature of 30 °C. These choices were made with a typical banana transport in mind. Though the analysis could be done for other fruit, there are two reasons to choose for banana:

1. Banana is by far the most common fruit shipped in reefer containers: approximately 25% of all reefer container shipments carry bananas.
2. Only in the banana trade it is common practice to not precool the cargo prior to container transport, hence the initial temperature of 25 °C, which is equal to the usual harvest temperature of bananas.

The differential equations of the physical model were integrated using matlab's ode45 function, which uses an explicit Runge-Kutta (4,5) formula, the Dormand-Prince pair. It is a single-step solver – in computing $x(t_n)$, it needs only the solution at the immediately preceding time point, $x(t_{n-1})$. The numerical accuracy was verified by running the simulation twice, once for default tolerances and once for very stringent tolerances, and visually verifying that there were no notable differences. Figure 5 till Figure 8 visualise the simulation results in multiple ways.

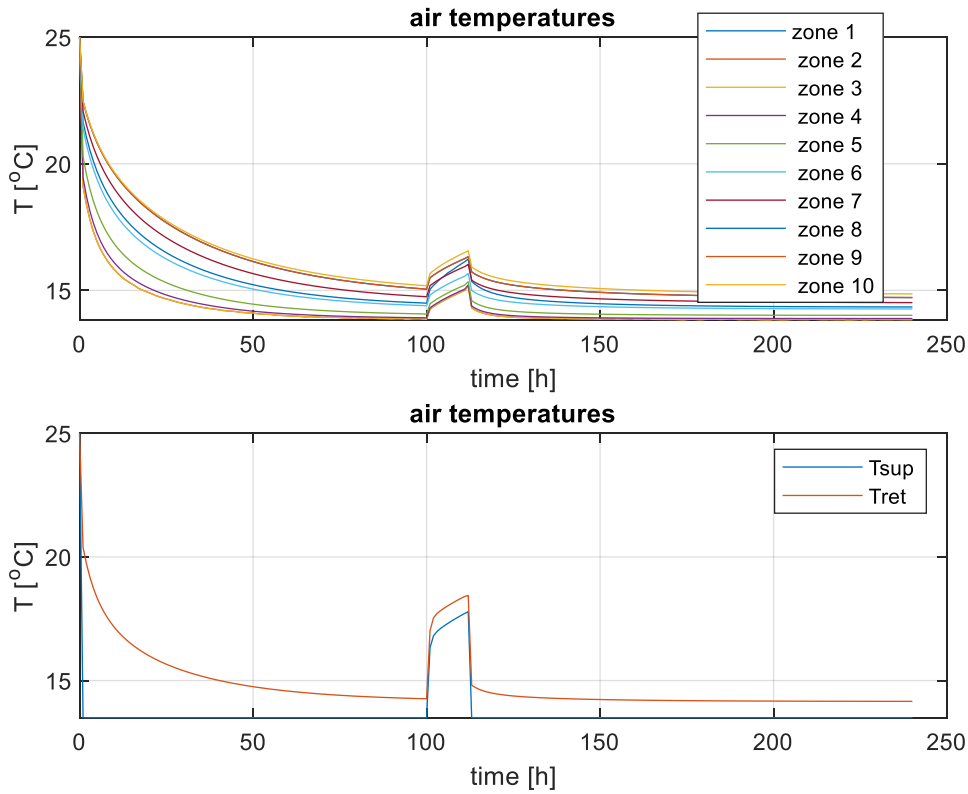


Figure 5 *time series plots of the simulated case. Presented are the air temperatures of each zone in the top figure, and the temperatures of supply and return air in the bottom figure*

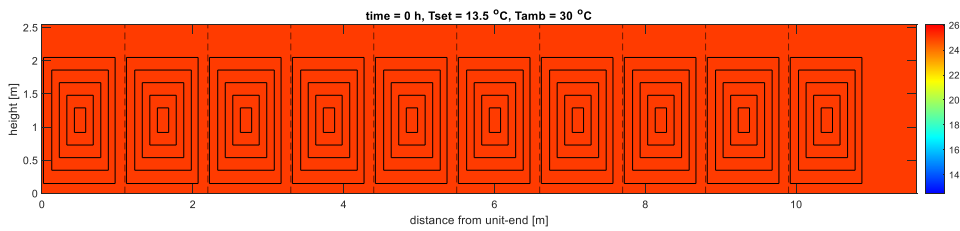


Figure 6 *contour plot of all simulated temperatures at initial time 0 h.*

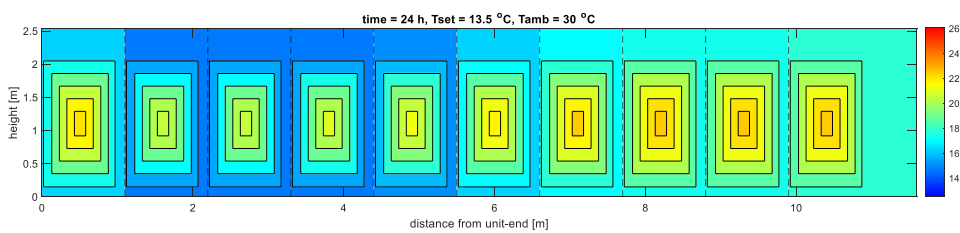


Figure 7 *contour plot of all simulated temperatures at time 24 h.*

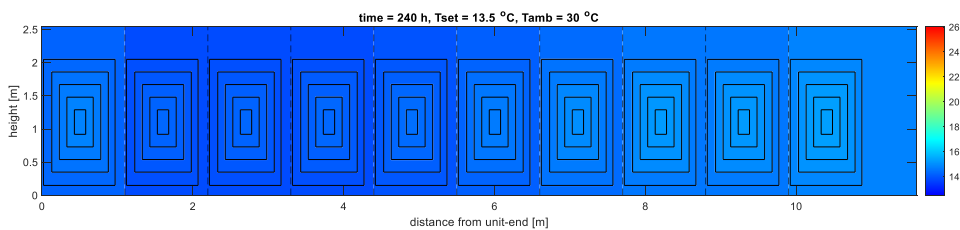


Figure 8 *contour plot of all simulated temperatures at final time 240 h.*

Though the physical model has not been validated explicitly, the simulation outcomes match reasonably well with multiple experiences, such as:

1. It takes multiple days before cargo temperature pulldown is completed (Figure 5a), like the authors observed many times in banana shipments.
2. During power-off periods temperatures rise about 0.1 °C/h (100 < t < 112 in Figure 5a), while practitioners assume 0.25 °C/h as a rule of thumb for reefer loads in general (most reefer loads are carried at temperatures lower than 13.5 °C, and will therefore heat faster during power-off).
3. In steady state the warmest pallets occur at the door-end, like measured in Lukasse et al. (2021a).
4. During power-off periods supply and return air temperature rise much faster than cargo space temperatures (Figure 5), and after restoring power supply all air temperatures rapidly return to the level prior to the power-off period. This corresponds with what the authors observed many times in practical shipments.
5. Pallet centres are warmer than the outer layers of pallets, also in steady state. This makes sense as it is hard to remove heat from pallet centres, where the air flow is nihil. Also, this corresponds with what the authors observed many times in practical shipments.

4.2 The studied sensor-placement methods

The two evaluated sensor-placement methods are:

1. Random.
2. Deterministic placement of 2 sensors: one in the bottom (layer 5) of the coldest pallet (zone 2) and one in the centre (layer 1) of the warmest pallet (zone 10).

What exactly does random mean in sensor-placement method 1? Random in the (X,Y,Z)-coordinates of the cargo. All randomly generated positions are based on uniform distributions of the (X,Y,Z)-coordinates between minimum and maximum bounds. In a uniform distribution all numbers are between the minimum and the maximum bounds and, as opposed to a normal distribution, all numbers between the minimum and maximum bounds are equally probable.

4.3 Evaluation criteria

The evaluation criteria are based on the difference between the cumulative distribution functions (CDFs) of the physical model output and the statistical model output. Section 3 explains how the CDF of the statistical model is calculated. The assessment of the CDF of the physical model output at time t involves the following steps. The physical model simulates all cargo temperatures, by dividing the cargo in 50 volume elements: n_{zones} zones within each zone a pallet with n_{layers} layers, where $n_{zones} = 10$ and $n_{layers} = 5$. Not each volume element represents an equal share of the cargo, because the volumes of the layers in a pallet load model differ (immediately visible in e.g. Figure 7). Therefore, a CDF of simply the 50 predicted temperatures would be an unbalanced representation of the cargo's temperature distribution. For a balanced representation of the cargo's temperature distribution the CDF of the 50 *volume-weighted* predicted temperatures is needed. Let $V(v)$ be the vector of the 50 volume elements, where each cargo volume element has a cargo temperature $T_v(t)$. Then

$$F_{phys}(T(t)) = \frac{1}{\sum_{v=1}^{50} V(v)} \sum_{v=1}^{50} ((T_v(t) \leq T) \times V(v)) \quad [-] \quad (28)$$

where $T(t)$ is defined as the vector of temperature values at which $F_{phys}(T(t))$ is evaluated. This study used:

$$T = \left[-10, \min_{v=1, \dots, 50} T_v(t) - 0.1, T_1(t) \dots T_{50}(t), 40 \right] \quad [^{\circ}\text{C}] \quad (29)$$

with $T_1(t) \dots T_{50}(t)$ the calculated temperatures of the model's 50 volume elements, sorted in ascending order. As cargo temperatures evolve over time the cumulative distribution functions of both the physical model and the statistical model evolve over time.

Figure 9 till Figure 11 illustrate this by means of examples. In this example the statistical model is based on two randomly placed sensors. Figure 9 shows that at time 0 no cargo temperature is above 25 °C and no cargo temperature is below 25 °C, exactly as visualized in the contour plot in Figure 6. In that situation the statistical model perfectly matches the physical model (red and blue curves in Figure 9 coincide). After 24 hours the cargo temperatures are much more diverse (see contour plot in Figure 7): *e.g.*, according to the physical model 33% of the cargo is colder than 17.4 °C (Figure 10). In this situation of diverse cargo temperatures, it is more difficult for the statistical model to match the physical model, resulting in a relatively large difference between the two CDFs (Figure 10). After completion of pulldown all cargo temperatures are at, or just above, setpoint (Figure 8). In these more homogeneous temperatures, it is easier again for the statistical model to match the physical model, resulting in a smaller difference between the two CDFs (Figure 11). According to the physical model's CDF then the coldest cargo is 13.9 °C and the warmest is 15.4 °C (Figure 11), which corresponds well with the colours in the contour plot (Figure 8).

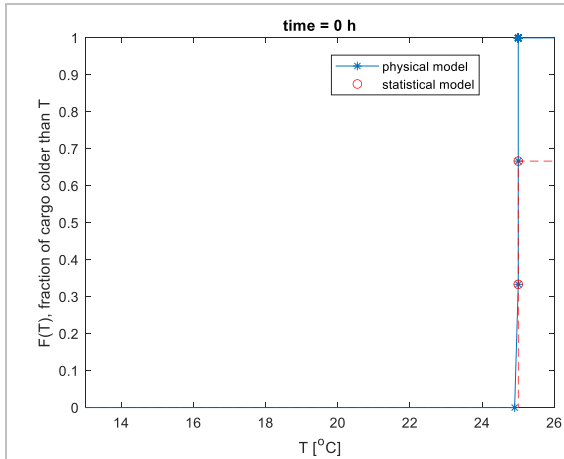


Figure 9
CDF of both models at initial time 0 h.

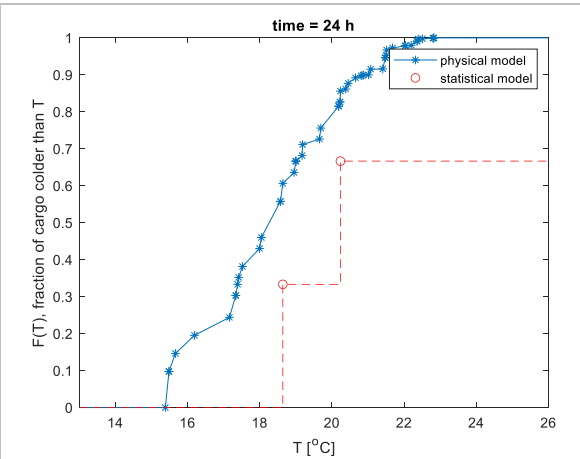


Figure 10
CDF of both models at time 24 h. (halfway pulldown)

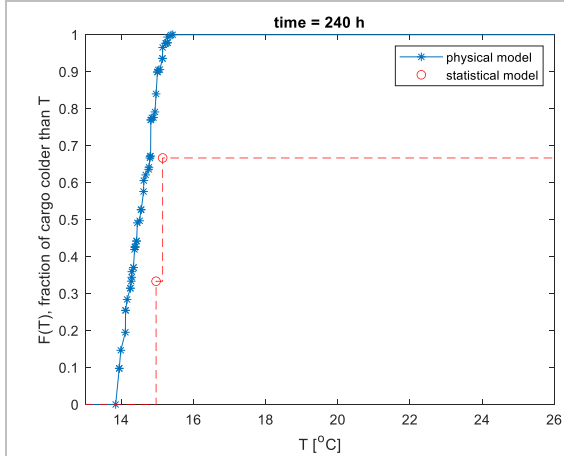


Figure 11
CDF of both models in final steady state (t = 240 h)

Under the assumption that the physical model representation of the container is sufficiently accurate, it is now possible to test if a randomly placed set of a specific amount of temperature probes is sufficient to reconstruct this physical representation. This is a statistical challenge, however, since statistics are most commonly used for null-hypothesis difference testing, where one assumes that two temperature distribution are similar, unless proven otherwise.

The problem of random sensor placement, where a distribution from the random sensor temperatures is compared to the actual temperature distribution found with the physical model, is a form of equivalence testing, where we assume the random sensor temperatures do not match the actual temperature distribution and hope to reject this null-hypothesis with a statistical test. For difference testing, the Kolmogorov-Smirnov (KS) test can be used to test if two distributions, considered the same, are in fact different.

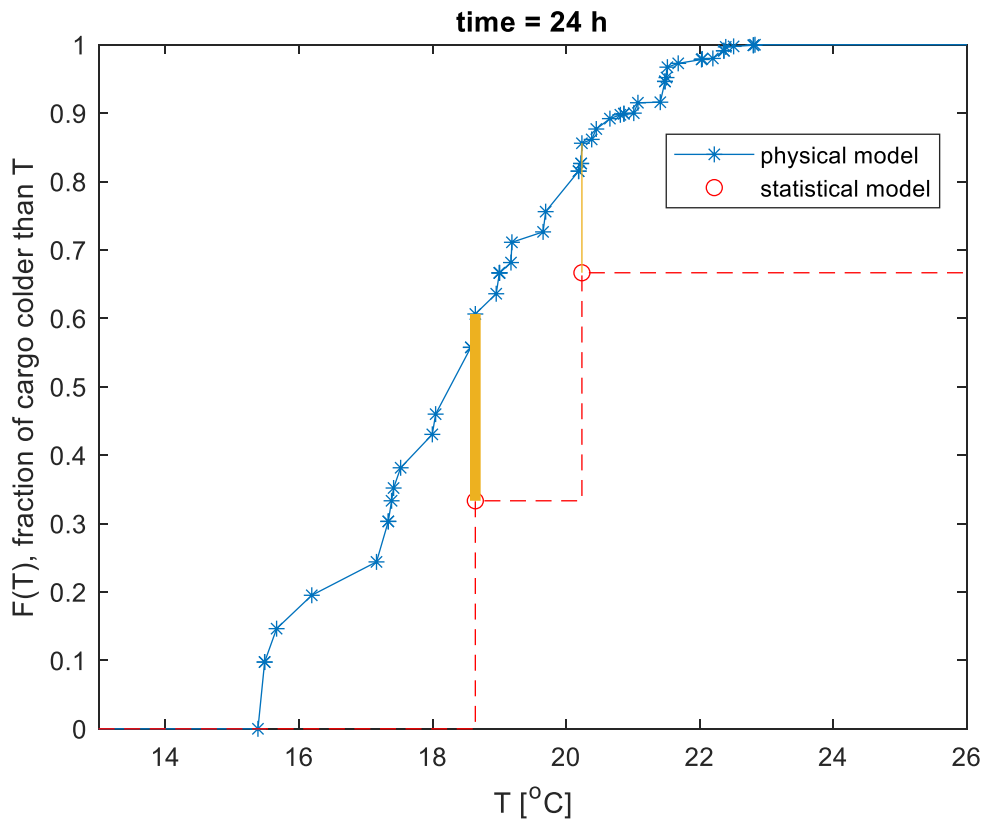


Figure 12 *cumulative distributions of temperature in a container, where the continuous distribution (blue) is the true temperature distribution in the container as found with the physical model, and the discrete distribution (red) derived from a single randomly drawn configuration of 2 temperature sensors from all possible sensor locations in the 3D-container*

The KS-test takes the largest absolute difference between both distributions (thick orange line in Figure 12), from which the chance is calculated that the randomly measured temperatures differ from the true temperature profile. It may then happen that, based on the KS-test, it cannot be concluded that both distributions are different. This does not mean these are the same. Hence the KS-test cannot be used to determine if the random sensors can accurately reconstruct the actual temperature profile (test if sensors are equivalent to true profile). However, the differences between both distributions do contain information about how close the random sensors can determine the actual temperature profile. While least squares of absolute errors are conventionally used as a measure for similarity of two samples, for cumulative distributions the horizontal error gives more insight, as it is a measure of error in temperature. For a given percentage, e.g. 33%, the physical model indicates that 33% of the container is colder than 17.4 °C, whereas the single random configuration of sensors of Figure 13 indicates 33% of the container is colder than 18.6 °C, thus both distributions show a horizontal error of 1.2 °C in this example.

The selected evaluation criterion is the maximum absolute (horizontal, *i.e.* temperature) error between the cumulative distribution functions (CDFs) of the physical model output and the statistical model output. It is evaluated at three time instants:

1. Pulldown: at time $t = 24$ h, in the midst of temperature.
2. Steady state: at time $t = 240$ h, in steady state.
3. Full trip: time-averaged over the full trip, from time zero till 240 hours.

These three evaluation criteria are explained in further detail below. The maximum absolute error MAE at time t (evaluation criteria 1 and 2) is calculated as

$$\text{MAE}(t) = \max_s \left| F_{phys}^{-1} \left(F_{stat} \left(T_{measured}(s, t) \right) \right) - T_{measured}(s, t) \right| \quad [^{\circ}\text{C}] \quad (30)$$

where $F_{phys}^{-1} \left(F_{stat} \left(T_{measured}(s, t) \right) \right)$ is the temperature $T_{phys}(t)$ at which $F_{phys}(T_{phys}(t))$ equals $F_{stat}(T_{measured}(s, t))$. It is found by linear interpolation between the two nearest data pairs ($T(t); F_{phys}(T(t))$) assessed in eqn. 28 and 29. Eqn. 30 boils down to assessing the length of the longest (bold) horizontal orange line in Figure 13.

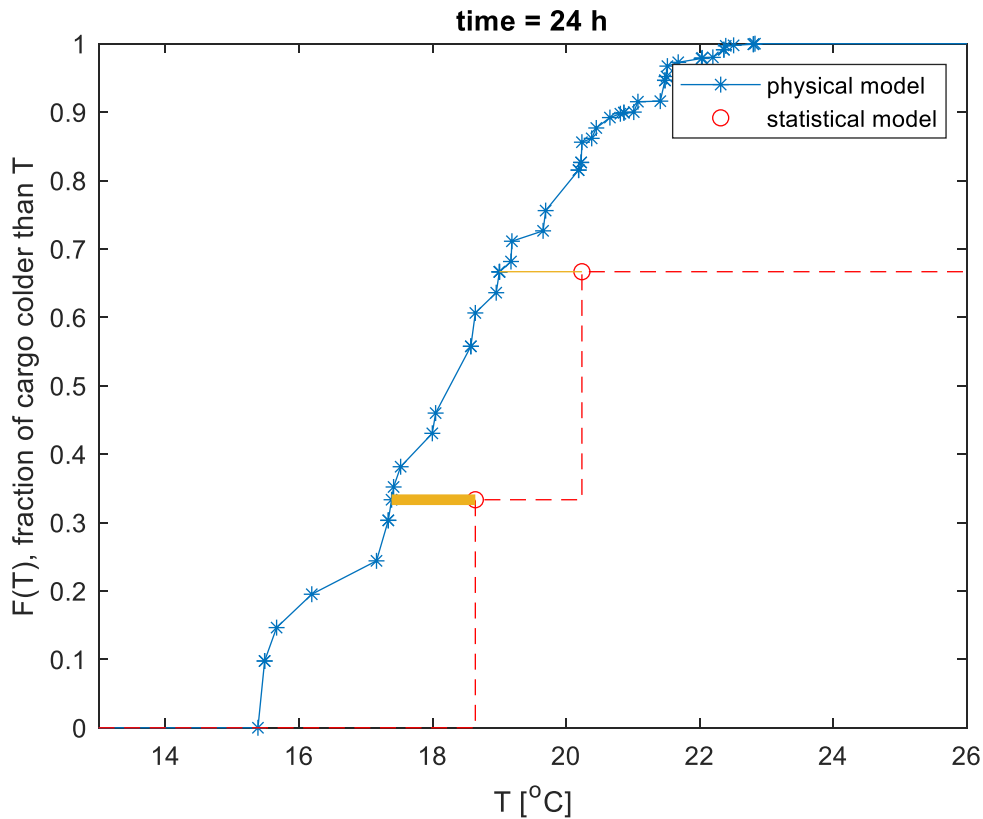


Figure 13 example of cumulative distribution functions of physical model, statistical model, and the difference (horizontal orange lines)

Evaluation criterion 3 (full trip) is the trip-averaged value of the MAE(t) as defined in eqn. 30. It is calculated as

$$\overline{\text{MAE}}(t) = \frac{1}{241} \sum_{t=0}^{240} \left(\max_s \left| F_{phys}^{-1} \left(F_{stat} \left(T_{measured}(s, t) \right) \right) - T_{measured}(s, t) \right| \right) \quad [^{\circ}\text{C}^2] \quad (31)$$

For the case with two randomly placed sensors visualized in Figure 9 till Figure 11 the evolution of MAE(t) over time is depicted in Figure 14: MAE = 0 at $t = 0$ (Figure 9), then MAE reaches its highest value during pulldown (Figure 10) and then again a smaller MAE in the final steady state (Figure 11).

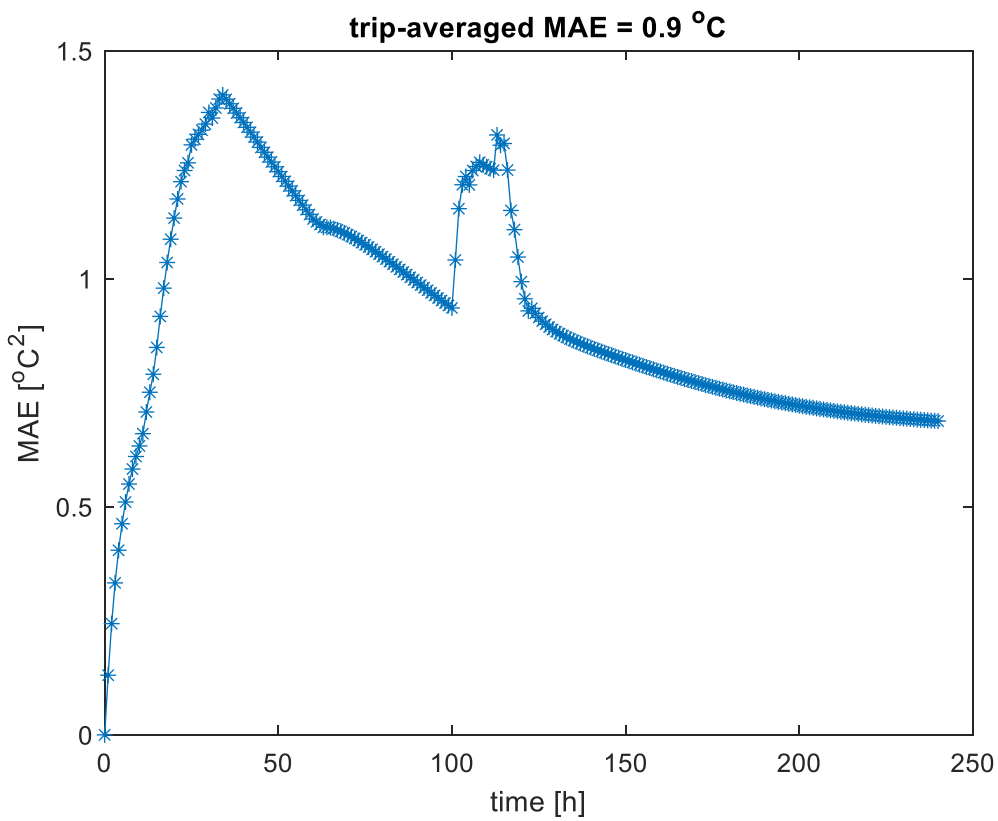
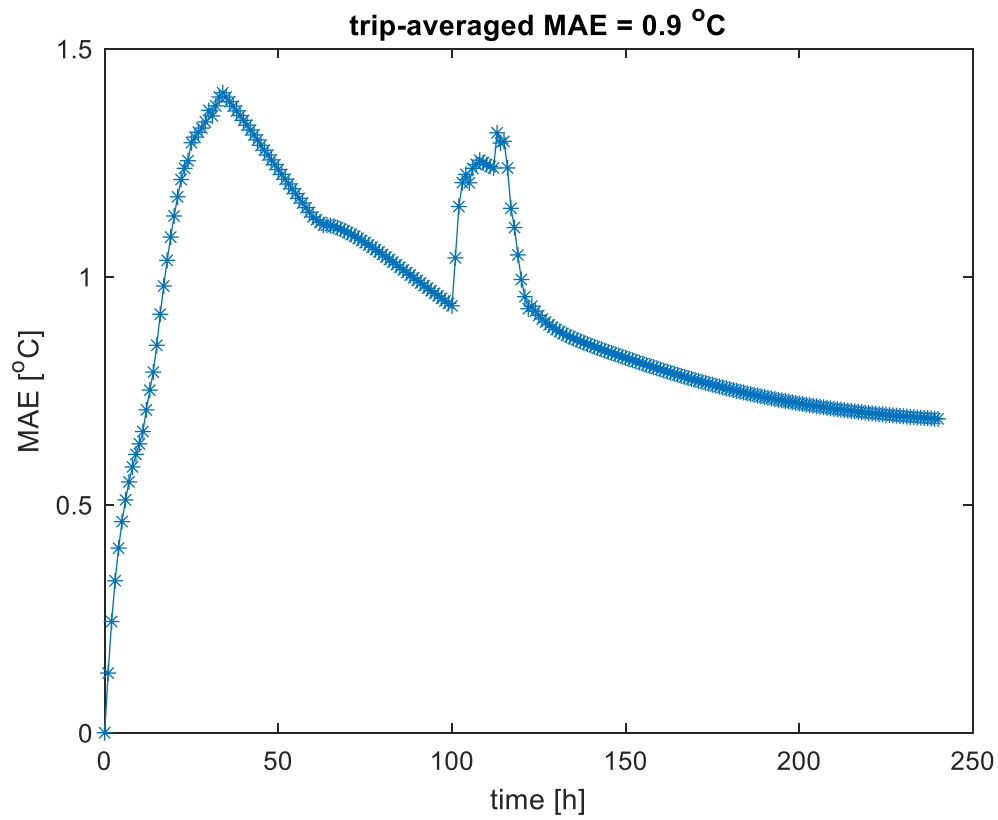


Figure 14 arbitrary example of MAE(t) as a function of time for a case with 2 randomly positioned sensors

Because the sensor placement is a stochastic process MAE(t) varies amongst realizations. Therefore, the three evaluation criteria are calculated for 1000 realizations with 2 till 40 sensors (39,000 realization in total). The results are presented in box plots (see e.g. Figure 15).

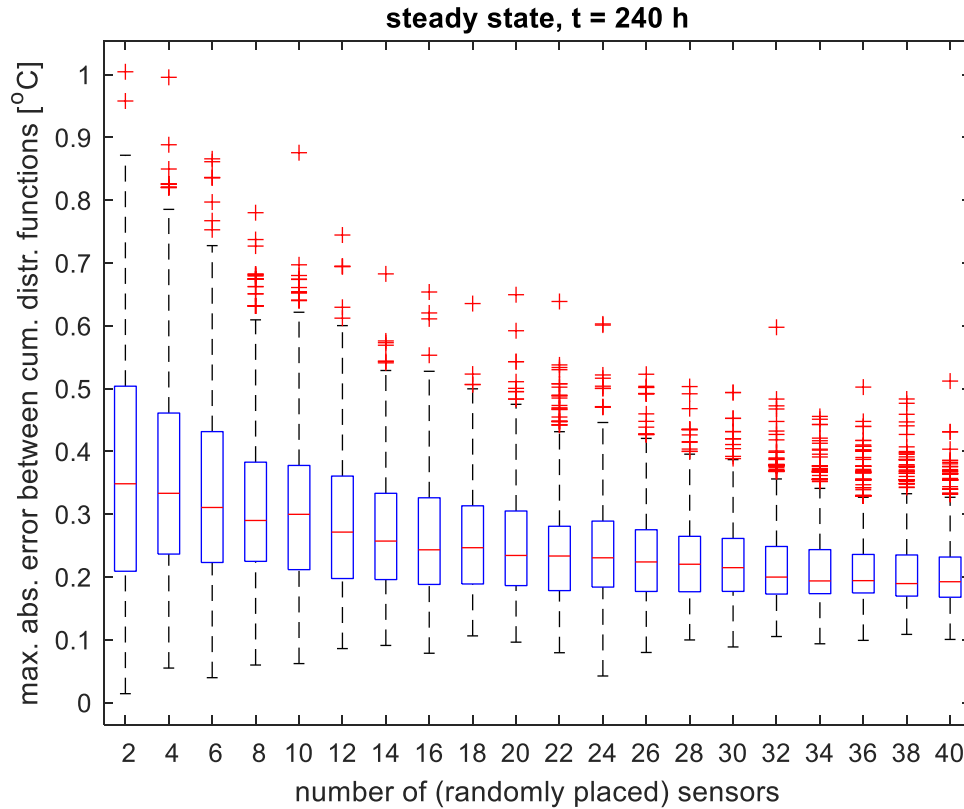


Figure 15 box plot showing MAE(t) in steady state for 1000 realizations with 2 till 40 sensors (39,000 realization in total)

On each box in Figure 15 the red central mark is the median, the lower and upper bounds of the blue box are the 25th and 75th percentiles, the black whiskers extend to the most extreme datapoints the algorithm considers to be not outliers, and the outliers are plotted individually (red plus). The maximum whisker length is set at 1.5x the distance between the Q1 and Q3 percentiles, where Q1 and Q3 are the 25th and 75th percentiles. Points are drawn as outliers if they are beyond that range. The whisker length of 1.5x(Q3-Q1) corresponds to approximately 99.3 coverage if the data are normally distributed. The worst case (top of upper whisker) and the Q3 error are interesting measures to assess the measured temperature error over the entire container based on these randomly placed sensors. If we place e.g. 2 sensors randomly 1000 times then in steady state the MAE(t) will hardly ever be larger than 0.87 °C (top of upper whisker), in 75% of cases MAE(t) will be less than 0.50 °C (Q3), and in 50% of cases MAE(t) will be less than 0.35 °C (median).

Although no statistical test of differences can be used to determine the optimal number of sensors, we can visualise the effect of the number of sensors on the expected temperature error between the actual temperature in the entire container (physical model output) and the temperature in the entire container as reconstructed based on a limited number of random sensors (statistical model output). For example, as indicated by Figure 15, placing 20 sensors would hardly ever result in a maximum absolute error of more than 0.47 °C (top of upper whisker) in steady state. In e.g. the example of Figure 16 the statistical model based on these 20 sensors indicates that 10% of the container is colder than 14.0 °C and 90% of the container is colder than 15.0 °C, we can derive how accurate this model based on these 20 sensors is. For this example, the maximum absolute error in the vast majority of cases of random sensor placement is $T(10\%) \leq 14.0 \pm 0.47$ °C and $T(90\%) \leq 15.0 \pm 0.47$ °C. By choosing a suitable allowable temperature error, a choice for number of sensors can be taken. A more pragmatic approach is to just qualitatively evaluate how the level of the upper whisker in the box plots evolves when the number of sensors increases.

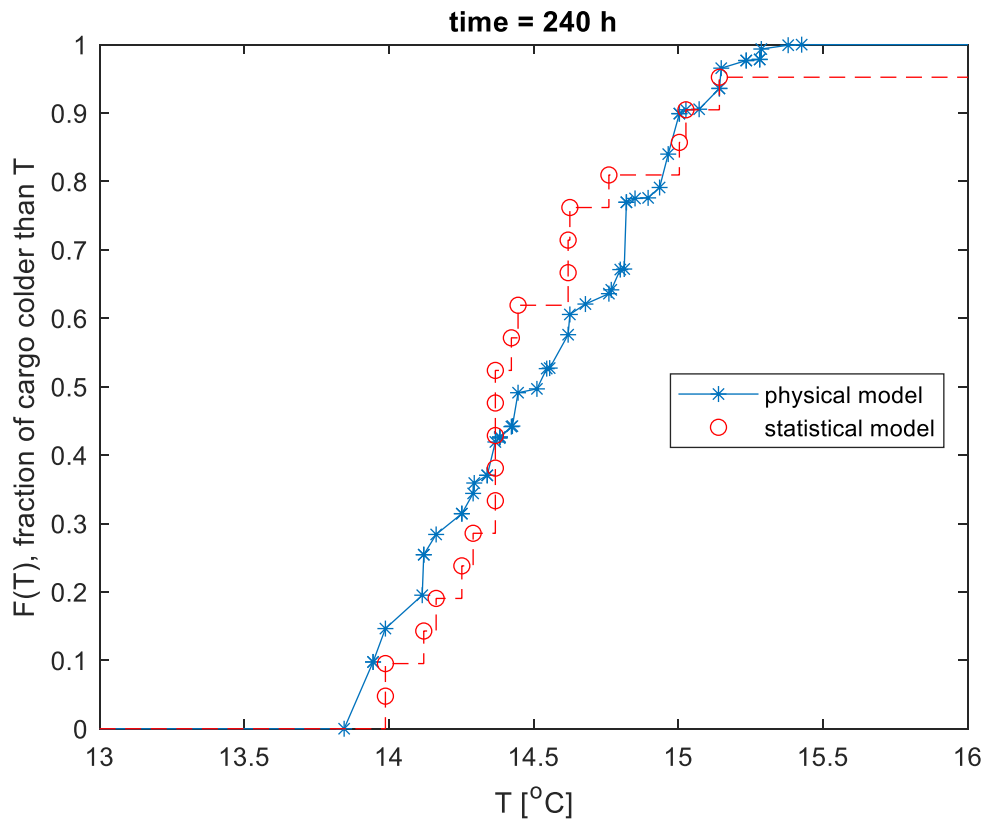


Figure 16 *example of $F_{phys}(T(t))$ and a realization of $F_{stat}(T_{measured}(s,t))$ for $N_{sensors} = 20$ at time $t = 240$ h*

4.4 Evaluated simulations

The studied transport scenario of section 4.1 has been taken as reference. The statistical model of section 3 is applied to this transport scenario for all sensor-placement methods described in section 4.2. The random sensor-placement method has been ran 1000 times for a number of 2 to 40 sensors: in total $1000 \times 39 = 39,000$ simulated sensor-placements. The deterministic sensor placement method with two sensors has been ran only once, as there is no stochasticity in this case.

5 Results

5.1 Random sensor placement

Figure 17 presents the Maximum Absolute Error at $t = 24$ h, *i.e.* in pulldown (evaluation criterion 1), for 1000 realizations of the random sensor placement method (section 4.2) for a number of 2 till 40 sensors. The next figure (Figure 19) presents the same information in the format of a box plot. The results for evaluation criteria 2 and 3 are only presented in the format of box plots (Figure 20, Figure 21).

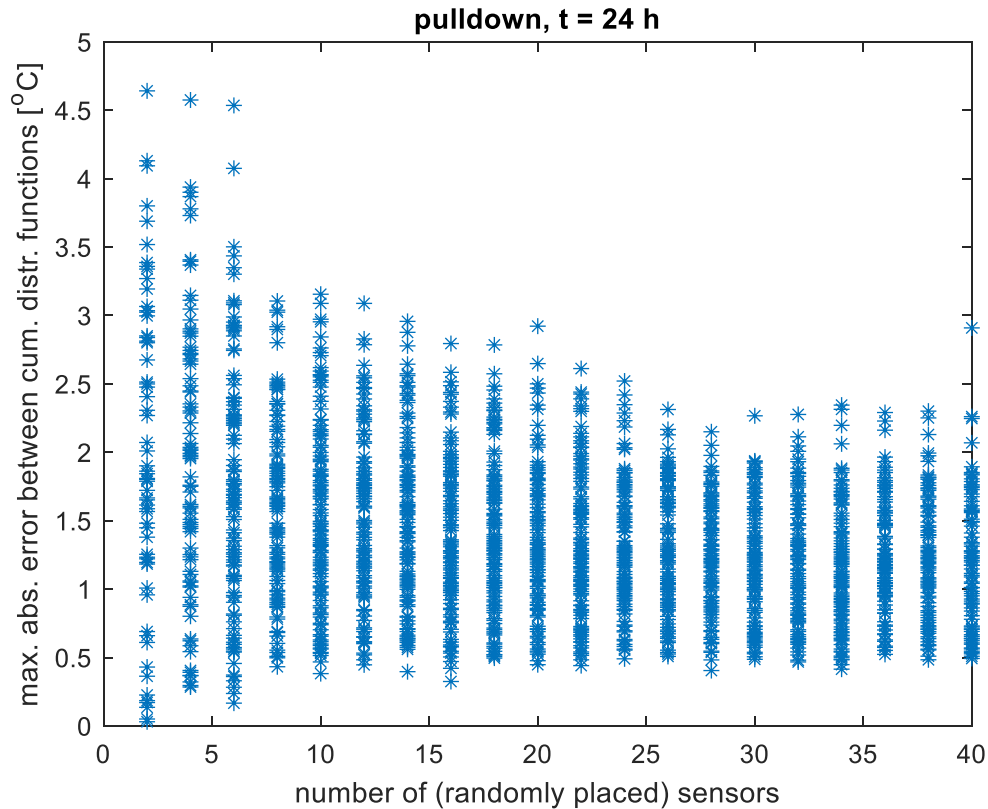


Figure 17 *MAE(t) at t = 24 h, i.e. in pulldown (evaluation criterion 1), for 1000 realizations of random sensor placement (section 4.2) for 2 till 40 sensors*

In the below box plots each box contains a central red mark indicating the median, while the bottom and top edges of the blue box indicate the 25th and 75th percentiles, respectively. The whiskers extend to maximally $1.5 \times (Q3 - Q1)$, yielding approximately 99.3 coverage if the data are normally distributed.

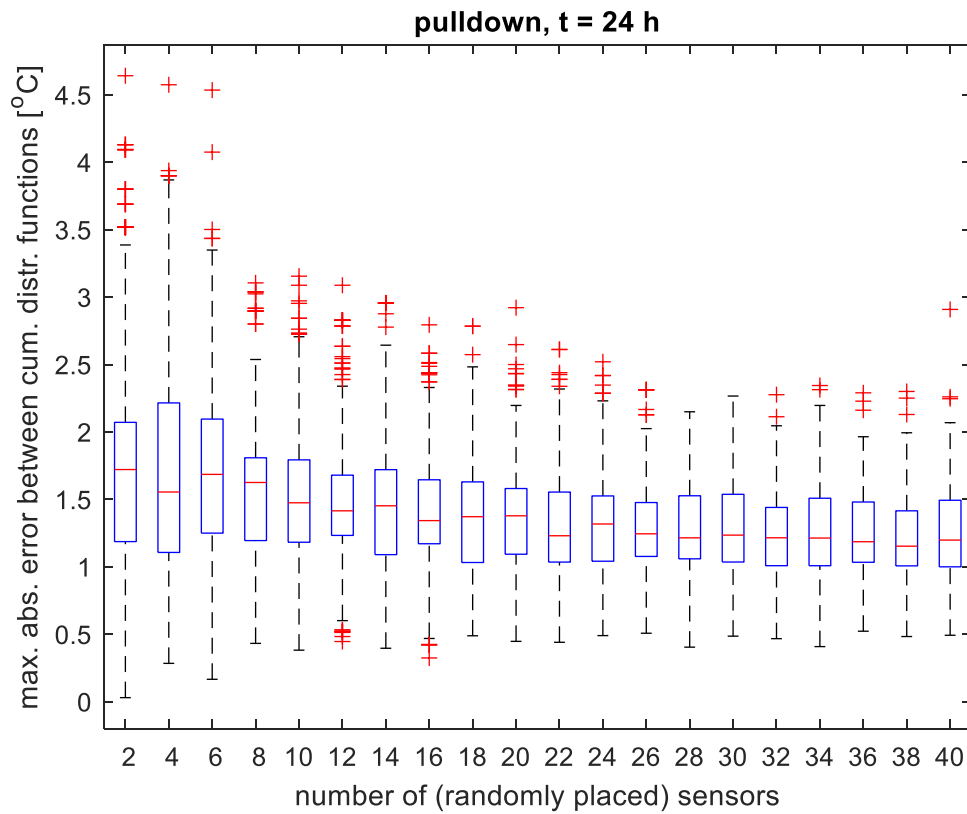


Figure 18 *box plot for MAE(t) in pull down, i.e. t = 24 h (evaluation criterion 1), for 1000 realizations of random sensor placement for 2 till 40 sensors*

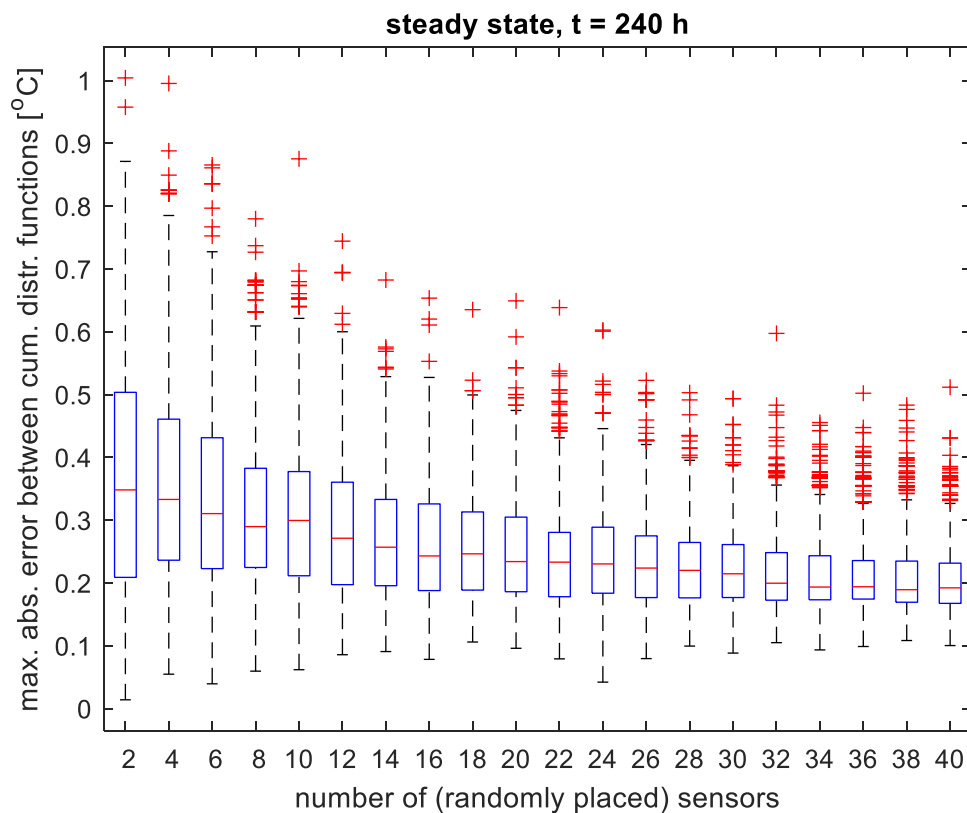


Figure 19 *box plot for MAE(t) in steady state (evaluation criterion 2) for 1000 realizations of random sensor placement for 2 till 40 sensors*

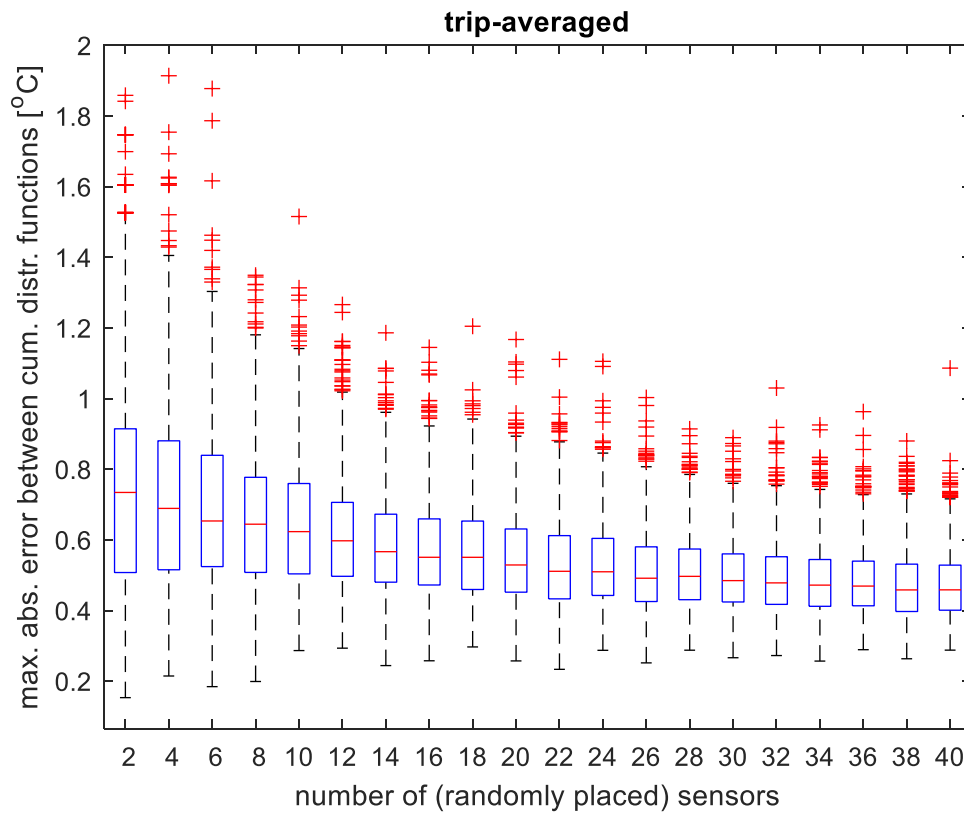


Figure 20 *box plot for trip-averaged MAE(t) (evaluation criterion 3) for 1000 realizations of random sensor placement for 2 till 40 sensors*

5.2 deterministic sensor placement

For the deterministic sensor placement method (section 4.2) with two sensors Table 8 presents the results.

Table 8 *simulation results for deterministic placement of 2 sensors*

| description of variable | value |
|---|---------|
| MAE(t) in final steady state (evaluation criterion 1) | 0.00 °C |
| trip-averaged MAE(t) (evaluation criterion 2) | 0.01 °C |

6 Discussion

6.1 Required number of sensors

How many randomly placed cargo temperature sensors are needed? The randomness causes a large uncertainty. As Figure 20 illustrate e.g. two luckily placed sensor may yield a trip-averaged MAE of 0.15 °C (end of lower whisker), while 40 sensors placed with bad luck may yield a worse trip-averaged MAE of 0.72 °C (end of upper whisker). As explained in section 4.3 the top edges of the upper whiskers in Figure 18 till Figure 20 are taken as a measure in answering the preceding question. Note that in Figure 18 (during pulldown) the MAE tends to be larger than in Figure 19 (steady state). This is simply the consequence of the presence of much bigger temperature gradients in the container during pulldown. Also note that there seem to be a relatively large numbers of outliers (red pluses) in the box plots. The used whisker length of $1.5 \times (Q3 - Q1)$ corresponds to approximately 99.3 coverage if the data are normally distributed. Why are so many realizations qualified as outliers? Because the 1000 realizations of MAE(t) for a specific number of sensors are not normally distributed. This has been verified by checking the histograms for specific sensor numbers (not shown). Whether or not the outliers are taken into account would not affect this report's conclusion, therefore no further action is taken.

Qualitatively evaluating how the level of the upper whisker in the box plots (Figure 18 till Figure 20) evolves, indicates that there is little benefit in using more than 30 randomly placed sensors. If one is satisfied with less accurate temperature estimates, for example because the carried cargo is less temperature-sensitive or the trip duration is shorter, then one may opt to use less sensors, accepting the risk of slightly worse temperature estimates. The methodology described in the final paragraph of section 4.3 may then be used to quantify the possible error margins to be anticipated.

6.2 Deterministic sensor placement

Is random placement a smart thing to do or is deterministic sensor placement superior? Deterministic sensor placement requires care, but proper deterministic sensor placement easily outperforms random sensor placement. As Table 8 illustrates only 2 sensors are needed to achieve $MAE(t_i) = 0.00$ °C and $\overline{MAE}(t) = 0.01$ °C, while Figure 18 and Figure 20 show that with even 40 randomly placed sensors the performance may well be worse.

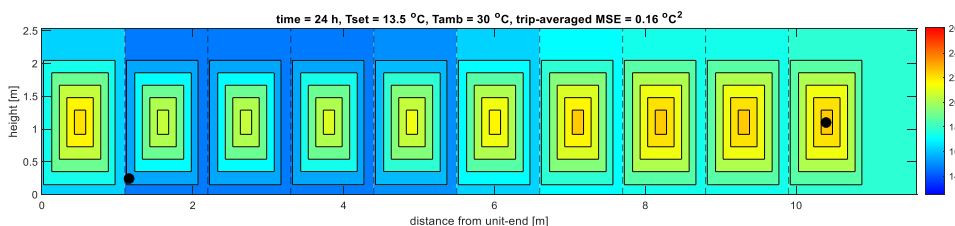


Figure 21 *dots indicate the positions of the two deterministically placed sensors yielding the performance reported in Table 8*

Note that the used deterministic sensor placement was inspired by the realization for $N_{\text{sensors}} = 2$ with the lowest trip-averaged MAE in Figure 20. Its sensor locations are illustrated in the figure below.

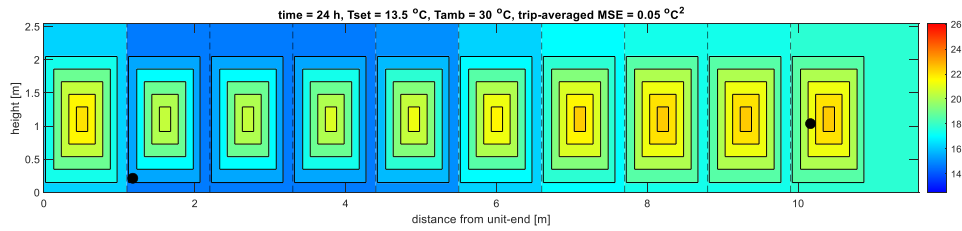


Figure 22 dots indicate the positions of the two deterministically placed sensors yielding the best performance for $N_{sensors} = 2$ in Figure 20

Note that there could still be reasons to use more, possibly randomly placed, sensors. Think *e.g.* of manufacturers of temperature-sensitive pharmaceuticals who routinely place at least one temperature sensor on each pallet load to record temperatures from moment of production till delivery at client (encompassing much more supply chain links than only container transport). If those sensors are there anyway, then they can easily be used as input to the statistical model. Another reason to use more temperature sensors is to be more robust against deviations between reality and this study's physical model. Such deviations may very well occur. *E.g.* when pallets are stowed less precisely: more or less direct contact with warm side walls, or when deviations from the presumed air flow distribution pattern occur, or when gradients occur in supply air temperature between left and right, possibly due to frost accumulation in the refrigeration unit.

6.3 Economic value

What is the economic value of a low trip-averaged Maximum Absolute Error (evaluation criterion 3, eqn. 31)? The question is insufficiently specific, and therefore impossible to answer. A low trip-averaged Maximum Absolute Error does mean that temperature recordings filtered through the statistical model give an accurate estimate of the evolution of the temperature distribution over time. The economic value of this information depends on many factors, such as the economic value of the cargo, the temperature sensitivity of the cargo, the duration of the trip, whether the collected information is actually actionable information, and the economic impact of such actions.

6.4 Applicability to refrigerated trailers

This study is limited to one simulated transport in a reefer container. Would the conclusion be different for a (single compartment) refrigerated trailers? No or hardly, because the physical model for the two cases is nearly identical. In reality the most significant difference is the use of bottom-air delivery in containers (Figure 1) versus top-air delivery in trailers (Figure 4). This has effect on vertical temperature gradients in the cargo space, but vertical temperature gradients are ignored in this study's physical model. With a richer model structure, taking into account vertical temperature gradients, the results might be a bit different. Yet, the authors do not expect a big difference.

6.5 Mechanistic or statistical model?

This study evaluates the estimation of all cargo temperatures from a limited number of measured cargo temperatures using a statistical model. Could better results be achieved by using a (partly) mechanistic model? Probably, but that approach is also much more complicated for multiple reasons:

1. The equations for processing the measurements will be (much) more complex.
2. Information about the transport equipment is needed.
3. Information about sensor locations is needed.

The statistical model is attractive for its simplicity: one simple model can be applied to any batch of fruit, and no further information is needed. A mechanistic (inverse!) model should be feasible, but the equations are (much) more complex (1), and require input of mechanistic information like evaporator fan capacity and control, supply air temperature, insulation value, and possible other parameters (2), to relate the model predictions to the sensor data the sensor locations need to be known (3).

7 Conclusions

The results indicate that there is little benefit in placing more than 30 randomly placed sensors per container load for the purpose of gaining a sufficiently accurate estimate of the temperatures of the complete cargo occurring during refrigerated transport in reefer containers, when using these recordings as inputs for a statistical model.

It is not to be expected that the situation will be a lot different for refrigerated trailers.

Care should be taken, as the above conclusions depend on many assumptions.

Random sensor placement is an ineffective sensor placement method, as two smartly placed sensors can be more informative than *e.g.* 40 randomly placed sensors. Smart sensor placement in a container is: one in the bottom of the coldest pallet (position 2 or 3 from unit-end) and one in the centre of the warmest pallet (door-end).

8 Recommendations

It is recommended to be more specific in formulating the purpose and application domain of temperature recording during transport. Purposes can *e.g.* be:

1. Gain a sufficiently accurate estimate of the temperatures of the complete cargo occurring during refrigerated transport.
2. Prove that no single cargo item in a pharmaceutical shipment experienced a temperature excursion during transport.
3. Prove that all temperatures staid below a certain threshold value during shipments according to USDA cold treatment protocol for quarantine purposes.
4. Collect some data that could serve as evidence in case cargo claims arise.

Also the application domain matters:

1. Whether or not the cargo is precooled affects the anticipated temperature distribution.
2. Is the cargo dead or not? *I.e.* could autonomous heat production persistently cause elevated temperatures in pallet centres?
3. The higher the temperature-sensitivity and the economic value of the cargo the more worthwhile it may be to accurately monitor the cargo temperatures during transport.

A more accurate physical model, taking into account vertical temperature gradients, can help to improve the accuracy of the outcomes, and give more specific advice.

Literature

Lukasse L. J. S., Staal M. G., Paillart M. J. M., Wildschut J. (2021a). Temperature uniformity and air flow distribution in a 40ft reefer container. Wageningen Food & Biobased Research report no. 2168 (confidential).

Lukasse L. J. S., Staal M. G., Wildschut J. (2021b). Temperature uniformity, air flow and fuel efficiency in a 45ft reefer container. Wageningen Food & Biobased Research report no. 2169 (confidential).

To explore
the potential
of nature to
improve the
quality of life



Wageningen Food & Biobased Research
Bornse Weilanden 9
6708 WG Wageningen
The Netherlands
E info.wfbr@wur.nl
wur.nl/wfbr

Report 2279

The mission of Wageningen University & Research is "To explore the potential of nature to improve the quality of life". Under the banner Wageningen University & Research, Wageningen University and the specialised research institutes of the Wageningen Research Foundation have joined forces in contributing to finding solutions to important questions in the domain of healthy food and living environment. With its roughly 30 branches, 6,800 employees (6,000 fte) and 12,900 students, Wageningen University & Research is one of the leading organisations in its domain. The unique Wageningen approach lies in its integrated approach to issues and the collaboration between different disciplines.

